International Journal of Smart Grid and Clean Energy

Design of a bidirectional power interface for V2G technology with smaller DC-link capacitance

Zirui Jia*, Liyuan Chen

College of Electrical Engineering, Zhejiang University, No.38 Zheda Road, Hangzhou (310027), China

Abstract

A configuration of a single-phase full-bridge AC-DC converter and dual active bridge (DAB) converter used in V2G (vehicle to grid) and G2V (grid to vehicle) technology is proposed in this paper. It can well realize the bi-directional energy fluidity. The numerous controllers can be designed by MATLAB SISOTOOL easily and quickly. And PLECS software is used to validate the function of the proposed system. In addition, a power decoupling method for this power interface is presented and verified. The simulation results show this configuration works well in V2G application and the DC-link capacitance could be reduced remarkably using proposed method.

Keywords: Bi-directional power interface, high power density, power decoupling, low harmonic distortion

1. Introduction

The basic concept of vehicle-to-grid power is used in EDVs (electric drive vehicles) to provide electric power to grid while vehicle is parked [1]. The EDV can be battery-electric vehicle, fuel vehicle, or plug-in hybrid vehicle. The stored energy in the battery and power converters in the EDVs can produce a 50 Hz AC voltage that power our homes and offices. When the electricity flows from EDVs to power lines, it is called V2G (vehicle to grid), while it is called G2V (grid to vehicle) conversely.

V2G technology has great advantage in terms of peak power, spinning reserves and regulation [2]. On-board power interface plays an important role, which must meet the demands of a bi-directional energy fluidity, rapid charge or discharge performance, and communication function of acceptance of charge or discharge command [3]. Besides, they should have the characteristics of high power density, high efficiency and intelligence. The topologies of bi-directional power interface can be divided into single-stage structures and two-stage structures [4]-[5]. Single-stage structures have disadvantages of complex control, isolation difficulty, large DC side capacitor, a lack of active current protection and so on. Two-stage structures are dominant in solving these problems, although they use more components.

For power electronic system design, PLECS simulation software can shorten cycle time of circuit development due to its high simulation speed. A system-level simulation design of a two-stage topology is carried out with MATLAB and PLECS Standalone in this paper. The first stage is a single-phase Full-Bridge AC-DC converter, and a Dual Active Bridge (DAB) DC-DC converter is the second stage [6]. Single-phase Full-Bridge AC-DC converter is to convert AC to DC bus voltage when charging the battery and to transform DC bus voltage to AC voltage for the grid when discharging. DAB works in the phase-shifted full-bridge mode to transform the bus voltage to charge the battery and conversely works in the full-bridge boost mode to convert the battery voltage to the bus voltage when discharging.

In this case, the bulk DC link capacitor between these two stages, which is necessary to store ripple power of two times the grid frequency, will be major barrier of improving power density. Research on performance of lithium-ion batteries shows that it does not exacerbate much operating with the current ripple at two times grid frequency [7]. With charging or discharging current containing low frequency

* Manuscript received July 10, 2013; revised August 17, 2013.
Corresponding author. Tel.: +86-136-7586-1895; *E-mail address*: jiazirui@zju.edu.cn.

ripple, the DC link capacitance could be reduced significantly, because the capacitors only need to filter the current ripple at switching frequency. Reference [8] gives the concept of sinusoidal charging. But the instantaneous power stored in the input inductor has not been considered, which affect the performance of power decoupling when input voltage is low.

This paper is organized as follows. Section 2 introduces system configuration and principle of operation. Design of the system is explained in Section 3. Since the proposed power decoupling method mostly effects the operation of DC-DC converter, Section 4 presented the operation principles of DAB with sinusoidal charging. Detailed simulated results have been discussed in Section 5. And the conclusive remarks are given in Section 6.

2. Principle of Operation

The overall operation of bidirectional converter could be divided into charging mode and discharging mode. Since the topology is bidirectional, the structure for charging and discharging are the same.

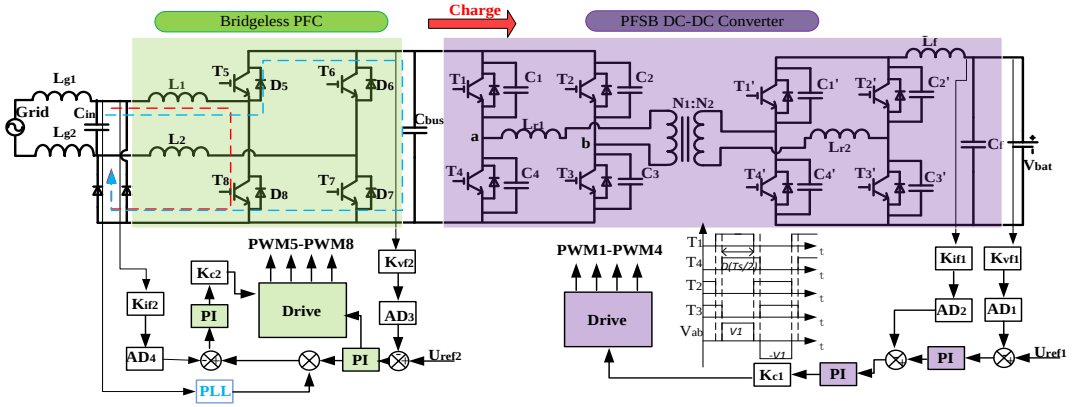

Fig. 1. Schematic and block diagram of control strategy in charging mode.

2.1. Charging mode

For charging mode, the electricity flows from the grid to the vehicle. Fig. 1 shows the schematic and block diagram of control strategy in charging mode. The circuit consists of the bridgeless PFC circuit and the phase-shift full-bridge circuit. The grid voltage is rectified into bus voltage, which charges the battery by the phase-shift full-bridge circuit.

The operation principle of bridgeless PFC is similar to that of the boost PFC circuit. But low common-mode (CM) noise interference and very high efficiency could be achieved in this dual boost bridgeless rectifier comparing to conventional boost PFC. Take positive half cycle for example, which is shown in Fig. 1. When T_8 is on, the current of L_1 is increased and when T_8 is off, the grid and the inductor together transfer the power to the load. The average current control method is adopted in this circuit. And the negative half cycle is similar to the positive half cycle.

For phase-shifted full-bridge converter, a two-loop control method with an inner current loop and an outer voltage loop is designed. The difference between reference voltage and sampling voltage through the voltage PI controller correction is a reference value of the inner current. The difference between this current and the sampling current pass through current PI controller and then it is multiplied by K_{c1}. Finally, PWM waveforms for the phase-shift full-bridge converter can be produced compared with triangular carrier. This two-loop control method can well charge the battery by constant current mode or constant voltage mode. The detail design of the control loop will be given in next part.

The control loop of PFC is usually polluted by second-order harmonic on DC bus voltage. In our proposed design, a notch filter is inserted in the feedback of voltage loop to solve this problem. The cutoff frequency of the notch filter is 100Hz and quality factor Q is 10.

2.2. Discharging mode

In discharging mode, the electricity flows from the vehicle to the grid. The circuit consists of a full-bridge Boost circuit, by which, the battery voltage is boosted to the bus voltage. Then the bus voltage is connected to the grid through a single-phase inverter circuit and feeds back energy to the grid. Fig.2 shows the schematic and block diagram of control strategy in discharging mode. For the DC-DC stage, a single-loop control method with the voltage loop is adopted to ensure it works in full-bridge boost mode. In the single-phase inverter, current reference is obtained by PLL of the grid voltage. And the PWM drive signal is produced by PI compensation of the current loop.

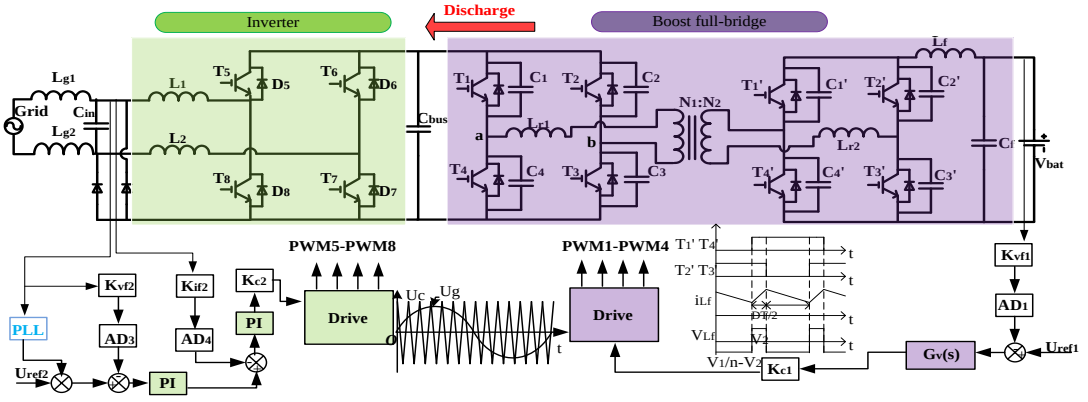

Fig. 2. Schematic and block diagram of control strategy in discharging mode.

3. System Design

The four compensation segments designed for the system are based on MATLAB integration toolbox, SISOTOOL. Root locus or Bode plots are used to adjust single-input and single-output feedback control system, combined with closed loop to adjust the gain and pole/zero points. The MATLAB toolbox will automatically generate the function of the compensation network, which shortens design cycle greatly.

The two-loop controller design is presented in detail. The block diagram of control system for phase-shifted full-bridge is shown in Fig.3, in which, K_{if1} and K_{vf1} is the sample coefficient of the system, K_{c1} is the reciprocal of the carrier peak, $G_{id1}(s)$ is the transfer function of the output current, $G_{i1}(s)$ and $G_{v1}(s)$ are the designed compensators. For the current inner-loop controller, the transfer function of the output current with duty cycle can be obtained from the small signal model shown as follow,

$$G_{id1}(s)=\frac{nV_{bus}}{\frac{R_L}{sR_LC_f+1}(L_fC_fs^2+\frac{L_f}{R_L}s+1)+4n^2L_{r1}f_s} \tag{1}$$

where n is the turns ratio of the transformer, L_f is filter inductance and C_f is filter capacitance, f_s is switching frequency, R_L is load resistance, and $L_{r1}$is the primary leakage inductance of the transformer.

The open-loop Bode plot is shown in Fig.4. It can be seen that low-frequency gain of the system is low, and the stability of system is poor with bad dynamic performance. So a compensation segment is needed. The Bode plot of $G_{id1}(s)$ added with the compensation transfer function is shown in Fig.5. The amplitude margin and phase margin are greatly improved. The phase margin reaches 82.5 ° meeting demand of the steady-state performance and dynamic performance. Final function of compensation network is as follow:

$$G_{i1}(s)=968.18\frac{1+0.00075s}{s} \tag{2}$$

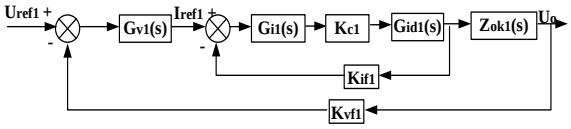

Fig. 3. Block diagram of control for phase-shifted full-bridge.

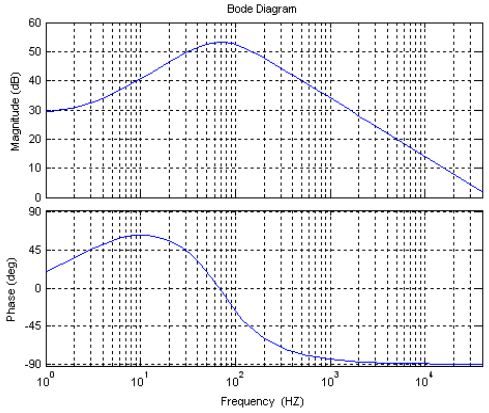

Fig. 4. Open-loop phase and frequency bode plots of $G_{id1}(s)$.

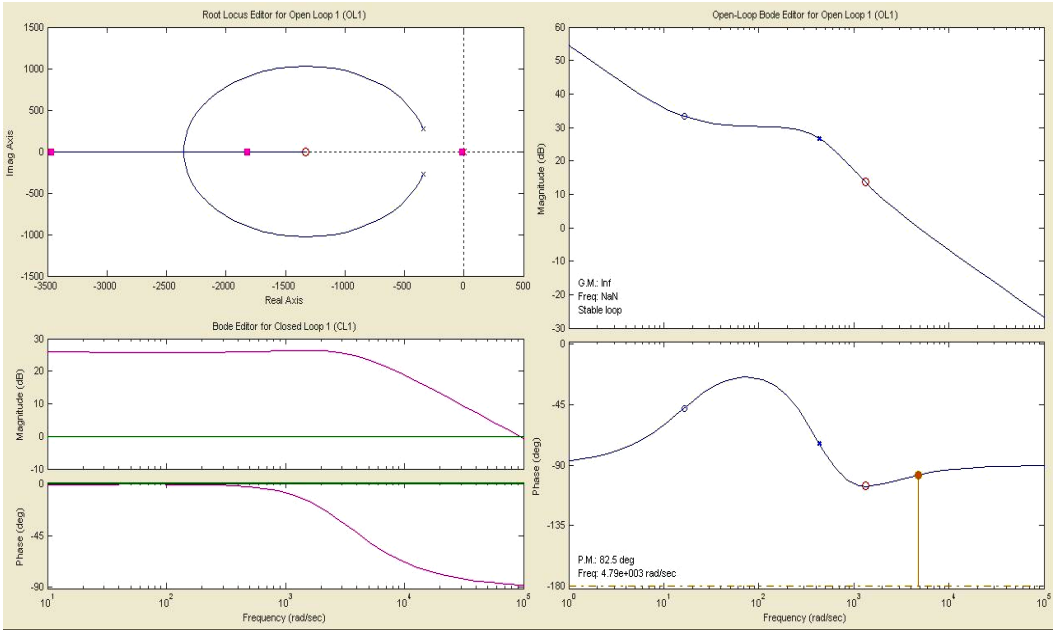

Fig. 5. Bode plots of $G_{id1}(s)$ added with the compensation link.

Similarly, voltage loop is designed after simplifying current inner-loop and the compensation transfer function is designed by SISOTOOL. Final compensation transfer function of voltage outer-loop is

$$G_{v1}(s) = 10.362\frac{1+9.3s}{s} \tag{3}$$

The compensation function of the controller for each circuit is summarized in Table 1. The two-loop PI control method is adopted for Bridgeless PFC. Two-zeros and two-poles controller design method is adopted for the full-bridge boost circuit, since there is a zero point in the left half plane, which may cause system instability. Circuit parameters of the system are shown in Table 2.

Table 1. The compensation function of the controller for each circuit

Circuit	Current loop	Voltage loop
Bridgeless PFC	$G_i(s)=0.3+0.176/s$	$G_v(s)=517+272/s$
Phase-shifted full-bridge	$G_i(s)=0.726+968/s$	$G_v(s)=96.37+10.36/s$
Full-bridge boost		$G_v(s)=-450\frac{(1+9\times10^{-5}s)(1+2\times10^{-4}s)}{s(1+4.8\times10^{-5}s)(1+3.3\times10^{-5}s)}$
Single-phase inverter	$G_i(s)=1.39+13.88/s$	

Table 2. Circuit parameters

Parameter	$L_1=L_2$	$L_{g1}=L_{g2}$	C_{in}	$N=N_p:N_s$	L_f	C_f	C_{bus}	V_{bus}	V_{bat}	f_s	L_{r1}	P_o
Value	3 mH	3 mH	20μF	1:1	1.2mH	4.7mF	4mF	380V	200~300V	20kHz	10uH	3kW

4. Power Decoupling Method

Assuming input voltage is $v_{in}(t)=V_{in}\cos(\omega t)$ and converter has unity power factor, the input power is:

$$p_{in}(t)=v_{in}(t)i_{in}(t)=\frac{V_{in}I_{in}}{2}+\frac{V_{in}I_{in}\cos(2\omega t)}{2} \tag{4}$$

Instantaneous power stored in the input inductor is:

$$p_{L_1}(t)=v_{L_1}(t)i_{in}(t)=-\frac{1}{2}\omega L_1 I^2{}_{in}\sin(2\omega t) \tag{5}$$

$$\begin{aligned} p_{bat}(t)&=p_{in}(t)-p_{L_1}(t)=\frac{V_{in}I_{in}}{2}+\frac{V_{in}I_{in}\cos(2\omega t)}{2}+\frac{\omega L_1 I^2{}_{in}\sin(2\omega t)}{2}\\ &=\frac{V_{in}I_{in}}{2}+\frac{\sqrt{(V_{in}I_{in})^2+(\omega L_1 I^2{}_{in})^2}}{2}\cos(2\omega t-\phi) \end{aligned} \tag{6}$$

where $\phi=\arctan(\omega L_1 I_{in}/V_{in})$. If all ripple power flows into batteries, charging current will behave in a sinusoidal waveform with a DC bias as:

$$i_o(t)=\frac{p_{bat}(t)}{V_{bat}}\approx\frac{V_{in}I_{in}}{V_{bat}}\cos^2(\omega t-\frac{\phi}{2}) \tag{7}$$

The ripple power at two times the line frequency in (7) will compensate ripple power in the input side. Thus, the DC link capacitors to store this ripple power can be eliminated theoretically. If V_{in} is 100V in our design, the phase-shifting angle ϕ could be 15.78°. So, ϕ shouldn't be omitted, especially when input voltage is low. A closed current loop is build to regulate the output current of DAB to be in the form of (7). As the battery voltage is constant, the voltage loop could be obsolete in practical condition. Full-digital controller gives the possibility to synchronize the control of both stages, and ease of monitoring the control and parameters in our work. Finally, the control scheme of DAB can be seen in Fig. 6. Phase-shifting module shifts the phase obtained from PLL of AC-DC. And then it is used to get reference current in the form of (7). Similarly, current loop of discharging mode is the same as Fig. 6 in this design.

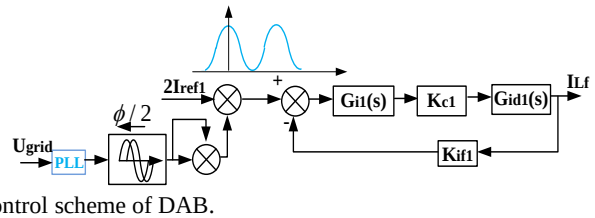

Fig. 6. Block diagram of control scheme of DAB.

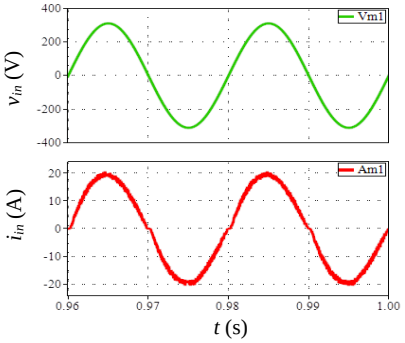

Fig. 7. Input voltage (green) and current (red) of PFC in full load.

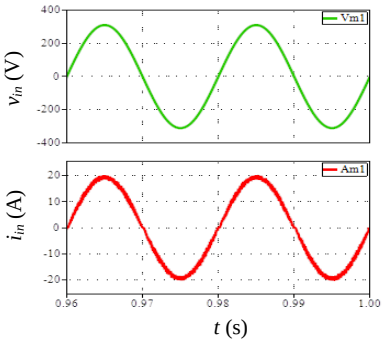

Fig. 8. Input voltage and current of PFC using novel control strategy.

5. Simulation Results

The whole system is simulated by PLECS Standalone. All control strategies are realized by C language.

When circuit works in charging mode, grid voltage is rectified through bridgeless PFC, followed by battery charging through phase-shift full-bridge circuit. Fig. 7 shows input voltage and current of PFC in full load. Due to zero-crossing distortion, THD of input current is about 5.2%. The same parameters are measured in circuit using duty-ratio feedforward control and notch filter. As shown in Fig. 8, THD is decreased to about 3.1% in the same condition. When changing half load to full load, input voltage, current and DC bus voltage is shown in Fig. 9. As it can be seen, ripple of DC bus voltage is about 6V in full load, while DC bus capacitance C_{bus} is 4mF. Using decoupling method we proposed, ripple of DC bus voltage is also about 6 V when C_{bus} is only 200μF. DC bus voltage and battery current is shown in Fig. 10.

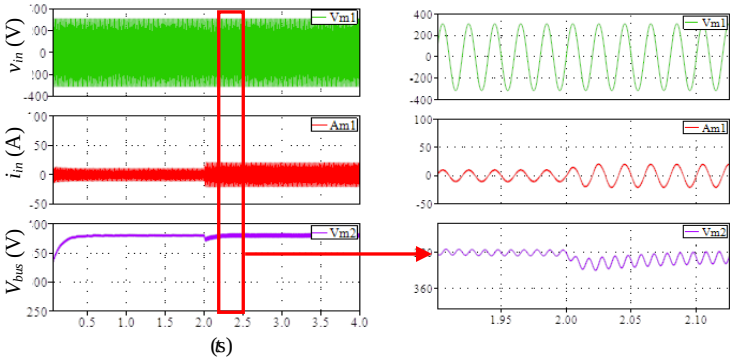

Fig. 9. Input voltage (green), current (red) and DC bus voltage (purple) when changing half load to full load (at 2s).

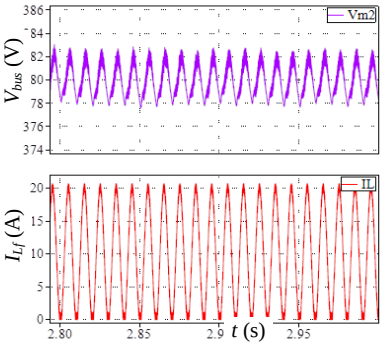

Fig. 10. DC bus voltage and battery current when charging (C_{bus} = 200 μF).

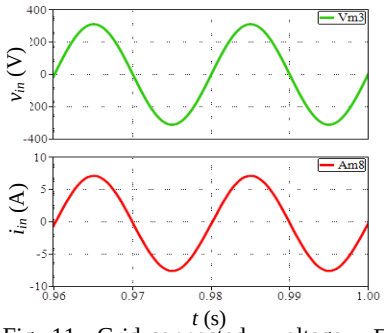

Fig. 11. Grid-connected voltage and current of inverter in full load.

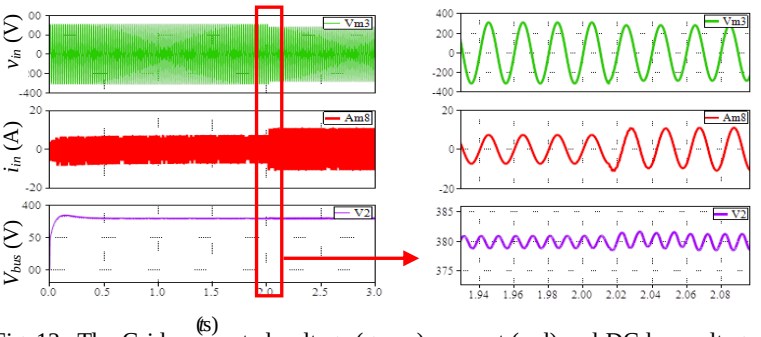

Fig. 12. The Grid-connected voltage (green), current (red) and DC bus voltage (purple) when changing grid voltage (220V to 200V).

In discharging mode, battery voltage is boost to bus voltage by full-bridge boost circuit, and then discharged to grid through inverter. The grid-connected voltage and current of inverter in the full load is shown in Fig. 11. THD of grid-connected current is about 1.1%. Fig. 12 shows the grid-connected voltage, current and DC bus voltage, when grid voltage is changing from 220V to 200V on the crest of wave. As it can be seen, the ripple of DC bus voltage is about 3V in full load, while C_{bus} is 4mF. When C_{bus} is only 200μF, ripple of DC bus voltage is about 4V in the same condition using the power decoupling method we presented. Fig. 13 shows the DC bus voltage and battery current in this case.

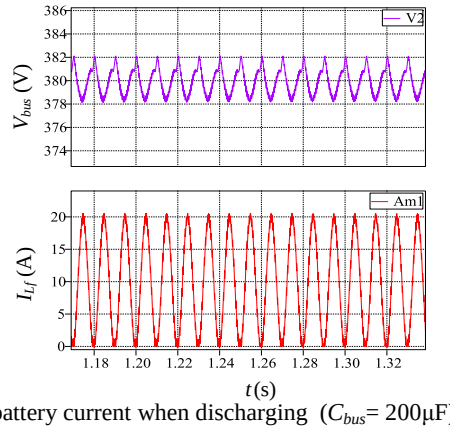

Fig. 13. The DC bus voltage and battery current when discharging (C_{bus}= 200μF).

6. Conclusion

In this paper, a configuration of a single-phase full-bridge AC-DC converter and DAB converter used in V2G technology is proposed. The function of the circuit achieving the charging or discharging mode is discussed and the PI controllers are easily designed by the use of SISOTOOL software. Furthermore, method of improving the THD of PFC input current and power decoupling is analyzed. Finally, based on MATLAB and PLECS, the simulation results are given to verify the function of the proposed system well. By using duty-ratio feedforward control, THD of PFC could be decreased. And DC link capacitor could be reduced to 200μF in 3 kW bidirectional power interface with sinusoidal charging and discharging.

References

[1] Kempton W, Letendre S. Electric vehicle value if integrated withthe utility system. In: Presented at Transportation Research Board,Washington, DC, 11 January, 1999.

[2] Kempton W, Kubo T. Electric-drive vehicles for peak power in Japan. *Energy Policy*, 2000; 28(1):9–18.

[3] Yilmaz M, Krein PT. Review of benefits and challenges of vehicle-to-grid technology. In: *Proc. of IEEE Energy Conversion Congress and Exposition*, 2012:3082-3089.

[4] Wong N, Kazerani M. A review of bidirectional on-board charger topologies for plugin vehicles. In: *Proc. of the 25th IEEE Canadian Conference on Electrical & Computer Engineering (CCECE)*, 2012:1-6.

[5] Fan Y, Xue Z, Han X. Bi-directionalconverting technique for vehicle to Grid. In: *Proc. of International Conference on Electrical Machines and Systems*, 2011:1-5.

[6] Segaran D, Holmes DG, McGrath BP. High-performance bi-directional AC-DC converters forPHEV with minimised DC bus capacitance. In: *Proc. of IECON 2011*, 2011:3620-3625.

[7] Uno M, Tanaka K. Influence of high-frequency charge-discharge cycling induced by cell voltage equalizers on the life performance of lithium-ion cells. *IEEE Transactions on Vehicular Technology*, 2011; 60(4):1505–1515.

[8] Xue L, Diaz D, Shen Z, *et al.* Dual active bridge based battery charger for plug-in hybrid electric vehicle with charging current containing low frequency ripple. In: *Proc. of IEEE 2012 Applied Power Electronics Conference*, 2013:1920-1925.